ORIGINAL PAPER

Symmetries and fuzzy symmetries of graphene molecules

**Shengkai Xing · Yun Li · Xuezhuang Zhao ·
Zunsheng Cai · Zhenfeng Shang · Xiufang Xu ·
Ruifang Li · Guichang Wang**

Abstract   In this paper, we will investigate the fuzzy layer group symmetries of two-dimensional (2D) periodic molecules. Here, we select several graphene molecules as typical examples to discuss. For these two-dimensional graphene molecules, their MO energies, symmetries and fuzzy symmetries are preliminarily studied. In addition, we especially make a detailed comparison between the zigzag and armchair graphene molecules. These studies will develop a theoretical framework that will help us to investigate the fuzzy symmetries of various layer group molecules as well as molecules with 3D periodic structure.

Keywords   Planar graphene molecules · Fuzzy layer group symmetry ·
Membership function · Irreducible representation component

1 Introduction

Fuzzy symmetry is a very interesting topic in theoretical chemistry and a few important results have been obtained [1–11]. In our previous papers, some research methods have been established to study the fuzzy symmetry characteristics of the molecule structures and molecular orbitals (MOs) [12,13] for the static and dynamic molecular systems [14–23]. For molecules possessing periodicity in one-dimensional direction, they are usually analyzed by using the cylinder group G_1^n [24,25], where n indicates the dimension of the space imbedding these one-dimensional (1D) periodic systems and generally is a positive integer and no more than three. However, in terms of real molecular structure, its periodicity in a certain direction is often incomplete (fuzzy),

S. Xing · Y. Li · X. Zhao (✉) · Z. Cai · Z. Shang · X. Xu · R. Li · G. Wang (✉)
College of Chemistry, Nankai University, Tianjin 300071, People's Republic of China
e-mail: zhaoxzh@nankai.edu.cn

G. Wang
e-mail: wangguichang@nankai.edu.cn

and we have done such studies on the molecules of polyyne [17], cumulative polyene [23], conjugate polyene [21,22], and their derivatives. These studies are about fuzzy point symmetry and fuzzy space periodic symmetry which is only involved for systems with 1D directional periodicity. In this paper, we will explore the molecules with fuzzy periodicity in two different directions in 2D plane, i.e. G_2^n systems [24,25]. Here, we select several graphene molecules as typical examples to investigate.

Graphene has attracted a great of attention because of its unique structural features and special physical and chemical properties in the past decades [26,27]. However, at one time, it has been regarded as a hypothetical structure or academic material, till Geim and Novoselov successfully isolated single sheets of graphene from the graphite crystals in laboratory in 2004 [28], which proved that graphene can exist by itself alone. Therefore, they shared the 2010 Nobel Prize in Physics. Graphene has many eximious properties, such as high thermal conductivity, strong mechanical strength, unique electrical property, and special electronic structure. So, it is regarded as an important nano-material to manufacture nano-electronic devices in the future. In the past decades, large numbers of article and review on graphene have been published, which were mostly concentrated in the molecule synthesis, spectroscopic properties, stability, and magnetism [29–34]. Here, several planar graphene molecules are taken as examples to analyze their π-MO energies, molecular symmetries, and fuzzy symmetries. These studies will lead to a better understanding of the microscopic structure and electronic properties of graphene, and help us expanding our molecular fuzzy symmetry studies from one-dimensional systems to 2D and 3D systems.

2 Molecular geometry and computational method

2.1 Molecular geometry of graphene

Graphene is a one-atom-thick sheet composed of the sp^2 carbon atoms arranged in hexagonal planar crystal, and it is a 2D honeycomb lattice periodic structure. Graphene structure is very stable and the C-C bond length is 1.42 Å. The connections between the individual carbon atoms are flexible, and the C-atom sheet will bend when the external force is applied on it. So, it does not need to re-arrange the C-atoms to adapt to the external force and maintain the structural stability [29–34]. Here, we will take quasi-graphene molecule $C_{200}H_{40}$ as an example to illuminate its molecular geometry and symmetry characteristics. As shown in Fig. 1, the molecule can be seen as quasi-graphene, except that its hexatomic rings are all benzene rings and the border C-atoms are saturated with hydrogen atoms. It contains $m \times n = 200$ ($m = 25$, $n = 8$) C-atoms. When m and n tend to infinite large, the molecule will form an infinite layer of graphene. This molecule exists periodic symmetries in two directions which is hexagonal plane lattice (namely, one of the five plane lattices) and the lattice point can be defined at the center of the benzene ring [24]. If such hexagonal plane lattice is disposed by Wigner-Seitz cell treatment, we can obtain the molecular structure arranged by C-atoms as shown in Fig. 1. The two independently basic periodic symmetry directions maybe selected differently. For example, one direction can be selected as the
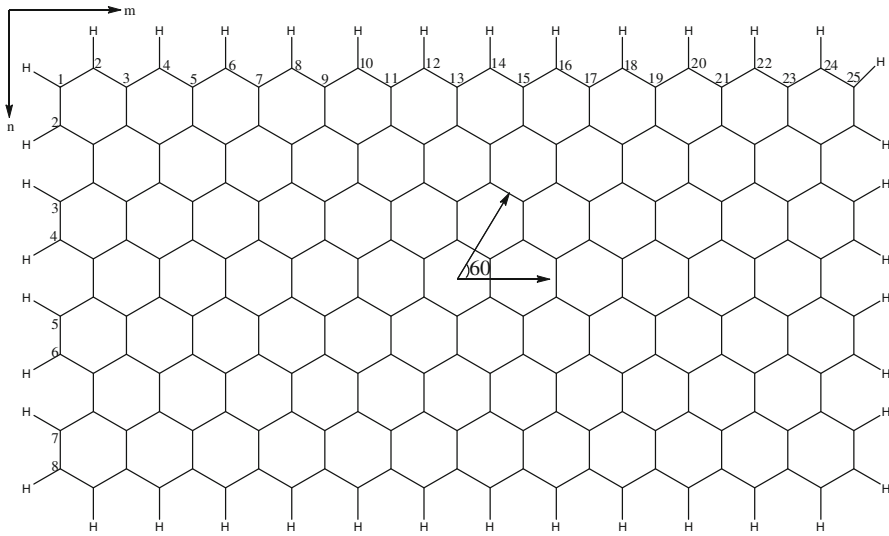
Fig. 1 Molecular structure of $C_{200}H_{40}$ composed of 200 C-atoms and 40 H-atoms ($m = 25$, $n = 8$)

horizontal direction, while the other one is selected in the direction forming a 60° angle with the horizontal direction (see Fig. 1).

According to Born-Karman approximation, when the number of lattice point of the one-dimensional point lattice is very large, its translational symmetry transformation is almost isomorphic with the corresponding higher rotational symmetry transformation. In Fig. 1, if we manipulate the horizontal translation to the corresponding rotational symmetry transformation and bond the left and right C-atoms (namely, the terminative C-atoms of both ends) together, we will obtain a zigzag carbon nanotube. Similarly, if manipulating the vertical translation into the corresponding rotational symmetry transformation and bonding the top and bottom C-atoms (terminative C-atoms in the same columns) together, these C-atoms can form an armchair carbon nanotube. Bonding the C-atoms by other methods, we can also obtain different carbon nanotubes with optical activity. On the other hand, when we manipulate both the horizontal and vertical transformations into the rotational symmetry transformation at the same time, these C-atoms will form a carbon 'nano-torus' [35]. This 'torus' is not a general torus in Euclidean space, and is related to a kind of specific symmetry which is different from the general point group symmetry and cylindrical group symmetry. Analysis of such torus symmetry has been discussed in other paper [36]. According to topology theory, the generators of the torus are made up of two independent translation orbit spaces [37]. Understanding of the above symmetry, it will help us to analyze the characteristics of the symmetry and fuzzy symmetry for such a kind of graphene molecules.

2.2 Fuzzy symmetry calculations of the molecular skeleton

For systems with cylinder group symmetry, which has the translational symmetry only in one direction, we just need to study its relevant symmetry or fuzzy symmetry on

this direction. However, for layer group systems possessing translational symmetry in two independent directions, the linear vector combinations of the two translational directions are usually also a kind of translational symmetry and the choices of the directions can be unlimited in principle. For graphene molecule, an appropriate choice is along the zigzag and armchair directions. In the following discussion, we generally investigated by this choice.

Taking the quasi-graphene $C_{200}H_{40}$ as an example, it is defined that the i row is counted from the top to bottom and the j column from the left to right. So, an arbitrary C-atom is labeled as $C(i, j)$, where i and j are integers in $[1, n]$ and $[1, m]$, respectively. For the H-atoms in the top and bottom lines, they can be marked as $H(0, j)$ and $H(n + 1, j)$ respectively, where the value of j is the same as that of the connected C-atom. Similarly, H-atoms in the left and right columns are marked as $H(i, 0)$ and $H(i, m + 1)$ respectively and the value of i is the same as that of the connected C-atom. Following this definition, any one graphene molecule contains $n \times m$ C-atoms and $(m - 1) + 2n$ H-atoms with the molecular formula $C_{mn}H_{(m-1+2n)}$. Any an atom $A(i, j)$ (A = C or H) in the molecule under the symmetry transformation $\hat{G}$ will change into atom $A(gi, gj)$, where $A(gi, gj)$ can be C, H or virtual atoms. Then, the atomic criterions of $A(i, j)$ and $A(gi, gj)$ atoms are defined as $Y(i, j)$ and $Y(gi, gj)$, respectively. According to the fuzzy symmetry theory, the membership function of the molecule under the symmetry transformation $\hat{G}$ is expressed as:

$$\mu_Z(\hat{G}) = \left[\sum_{i,j} (Y(i, j) \wedge Y(gi, gj)) \right] \bigg/ \left[\sum_{i,j} (Y(i, j)) \right] \quad (1)$$

where the values of i and j are integers in $[0, n + 1]$ and $[0, m + 1]$. For the virtual atom, its corresponding atomic criterion is 0; for non-virtual atom, the corresponding atomic criterion can be defined according to different requirements. For example, the molecular skeleton can take the atomic numbers as the criterion for its atoms. Thus, in formula (1), the denominator is actually the summation of the atomic numbers of all the atoms. For molecule $C_{200}H_{40}$, the denominator is $(6mn + m - 1 + 2n)$ and its value is 1,240, while the value of numerator portion in formula (1) is no larger than 1,240, the membership functions are no bigger than one.

Then, we will analyze the molecular skeleton membership function of molecule $C_{200}H_{40}$ about the translational symmetry transformation. We firstly investigate the membership function of translating l periodic lengths along the horizontal direction rightwards. For any one atom $A(i, j)$, it changes into $A(i, gj) = A(i, j + 2l)$ after translation l periodic lengths. For the molecular skeleton, the membership function of formula (1) changes into:

$$\mu_Z(\hat{G}) = \{n(m - 2l)Y_C + (m + 2n - 2l - 1)Y_H\} / \{nmY_C + (m + 2n - 1)Y_H\} \quad (2)$$

It can be seen that such membership function of molecular skeleton declines linearly with the periodic length 2l, and approaches to 1 with the increase of m. For example, in molecule $C_{200}H_{40}$, when translating one periodic length, its membership function is 1,142/1,240(about 0.921); even translation two periodic lengths, the membership

function is 1,044/1,240(about 0.842). It can be seen that if this molecule is treated with the general space translational group, the results will not be distorted too much.

If we omit the H-atoms in the quasi-graphene molecule, which is equivalent to investigate the graphite fragments, and the formula (2) can be reduced as:

$$\mu_Z(\hat{G}) = \{n(m - 2l)Y_C\} / \{nmY_C\} = (m - 2l)/m \tag{2-1}$$

For $C_{200}H_{40}$, its membership function of translating one periodic length is $23/25 = 0.92$; while that of translating two periodic lengths is $21/25 = 0.84$. We can see that the influence of H-atoms is very tiny. We can also make similar analysis for other direction translational symmetry transformation. On the other hand, for molecule $C_{200}H_{40}$, when we translate it along the upright direction (i.e. the armchair direction), its membership function of translating l' periodic lengths along the upright direction can be expressed as:

$$\mu_Z(\hat{G}) = \{m(n - 2l')Y_C + (m + 2n - 2l' - 1)Y_H\} / \{nmY_C + (m + 2n - 1)Y_H\} \tag{3}$$

From formula (3), we can see that the membership function of molecular skeleton about translational symmetry transformation also declines linearly with the periodic lengths 2l', while approaches to 1. Also for $C_{200}H_{40}$, when translating one periodic length along the upright (armchair) direction, its membership function is 938/1,240 (about 0.756). If we omit the H-atoms, the formula (3) can be reduced as:

$$\mu_Z(\hat{G}) = \{m(n - 2l')Y_C\} / \{nmY_C\} = (n - 2l')/n \tag{3-1}$$

Then, its membership function about translating one periodic length along the upright direction is $6/8 = 0.75$, which is very close to the value calculated by formula (3) when considering the H-atoms.

Comparing the membership function of translating 1 periodic length along the horizontal direction with that of along the upright direction, we can see that the former (0.92) is much bigger than the latter (0.75). This indicates that if $C_{200}H_{40}$ is treated with the general space translational group along the horizontal direction, the results will not be distorted too much, while it will be distorted somewhat along the upright direction. The reason can be found in the following presentation. In investigating the fuzzy one-dimensional periodic systems with limited size [17,21], we have indicated that when the characteristic size of one-dimensional system is ten times more than the translation length, the corresponding translational symmetry membership function is relative large ($>0.8 \sim 0.9$) and its symmetry can be approximately disposed by a perfect space group. For graphene molecule belongs to the fuzzy 2D system, we need to analyze the translational membership function along two different periodic directions. For molecule $C_{200}H_{40}$, the membership function of translating one periodic length along the horizontal direction (treated as zigzag graphene) is 0.92, while that of translating a periodic length along the vertical direction (treated as armchair grephene) is only 0.75. This is because the molecular size of the $C_{200}H_{40}$ is set with 12

periodic lengths expanding along the zigzag direction, while only 4 periodic lengths expanding along the armchair direction.

2.3 Fuzzy symmetry calculations of π-MO

The π-MO of graphene calculated by the computational chemistry program can be denoted as:

$$\Psi_\rho = \sum_{ja} \sum_{iao} a_\rho(ja, iao)\varphi(ja, iao) = \sum_{v=0}^{n-1} \Psi_\rho(v) \tag{4}$$

Then, the MO membership function can be obtained by the molecular orbital linear combination coefficients $a_\rho(ja, iao)$ of the LCAO-MO. Where $a_\rho(ja, iao)$ expresses the iaoth atomic orbital of the jath atom. The membership function of Ψ_ρ-MO about the $\hat{G}$ symmetry transformation is denoted as [12–15]:

$$\mu_Y(\hat{G}; \Psi) = \sum_{ja} \sum_{iao} \left(Y_{(ja,jao)} \Lambda Y_{(gja,gao)}\right) \bigg/ \sum_{ja} \sum_{iao} \left(Y_{(ja,jao)}\right) \tag{5}$$

According the fuzzy symmetry theory, $Y_\rho(ja, jao)$ in the above formula is chosen as the square of the molecular orbital linear combination coefficients $a_\rho(ja, iao)$ and its value is of course relative to Ψ_ρ.

All the molecular orbital calculations are performed on the Gaussian03 program [38] by using the HF/STO-3G method. We mainly discuss the fuzzy symmetry of π-MO about the space translational symmetry transformation along the zigzag direction and the armchair direction.

3 Results and discussion

Convenient for comparison and discussion, we analyze the molecular structures, π-MO energies and fuzzy symmetries of several zigzag and armchair graphene molecules with D_{2h} point group symmetry. In addition, several graphenes else with other symmetries are also studied to compare with the zigzag and armchair graphenes.

3.1 Zigzag graphene molecules

Primarily, we discussed four zigzag graphene molecules with D_{2h} point group symmetry: $C_{100}H_{32}$, $C_{84}H_{28}$, $C_{68}H_{24}$, and $C_{52}H_{20}$. Their geometrical skeleton structures are similar to that of molecule $C_{200}H_{40}$ (see Fig. 1). They all contain four lines ($n = 4$) of C-atoms, while the columns $m = (4i + 1$; where $i = 6, 5, 4, 3$) decrease in turn along the horizontal direction, similar as a group of homologues. These four molecules respectively contain $(4i + 1) \times 4$ C-atoms and form $m \times n = 4m$ π-MOs, in which the bonding occupied molecular orbitals (OMOs) and the anti-bonding vacant molecular
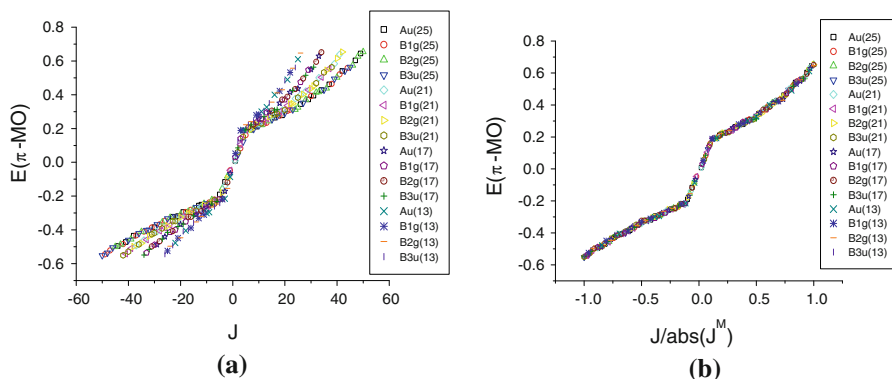
Fig. 2 π-MO energies of zigzag graphene $C_{100}H_{32}$, $C_{84}H_{28}$, $C_{68}H_{24}$, and $C_{52}H_{20}$. **a** π-MO energy versus J. **b** π-MO energy versus J/J^M

orbitals (VMOs) each account for a half. According to the group theory, those π-MOs of D_{2h} point group belong to some of the four irreducible representations: A_u, B_{1g}, B_{2g}, and B_{3u}. Calculated by Gaussian program at the STO-3G level, we find that the number of those π-MOs belonged to A_u and B_{1g} is both $(m-1)$, while that belonged to B_{2g} and B_{3u} is both $(m+1)$.

3.1.1 Symmetry characteristics of the MO energy in zigzag graphene

We denote the HOMO and LUMO as π-OMO-1 and π-VMO-1, the other bonding and anti-bonding π-MO are expressed as π-OMO-J and π-VMO-J, respectively. The suffix J denotes the serial number of π-MOs. So, its value of the frontier MO is 1, and the values of other π-MOs are 2, 3, ..., and $2m$ in turn. Then, the π-MO energies versus molecular orbital number J plots are drawn for the four zigzag graphene molecules and each shows an approximate italic "*S*-shaped" curve composed by the energy dots corresponding to π-MOs as given in Fig. 2a, where the abscissa is J, negative for the OMO and positive for the VMO, respectively. From Fig. 2a, we can see that the energy dots corresponding to OMO and VMO are segregated in two sets but close to each other, forming two separated branches. In addition, only small energy gaps exist between the OMO and VMO for all the molecules. We have pointed out that for some conjugated molecules, such kind of π-OMO and π-VMO branches are corresponding to the full band and the conduction band of one-dimensional crystals, and the gap is corresponding to the forbidden band gap [21,22]. So, it can be expected that a zigzag graphene molecule containing a large quantity of C-atom should have electrical conductivity, which is consistent with the known results [39].

These π-MOs all possess D_{2h} point group symmetry, belong to one of the irreducible representations (A_u, B_{1g}, B_{2g}, and B_{3u}), and are labeled by different symbols as shown in Fig. 2a. Furthermore, if we use the relative orbital number J/abs(J^M) instead of the orbital number J (J^M is the largest absolute value of J), the corresponding energy dots of the four graphenes fall into the same italic "*S*-shaped" curve as shown in Fig. 2b. Moreover, the dot distributions in Fig. 2a seem to hint certain rules,
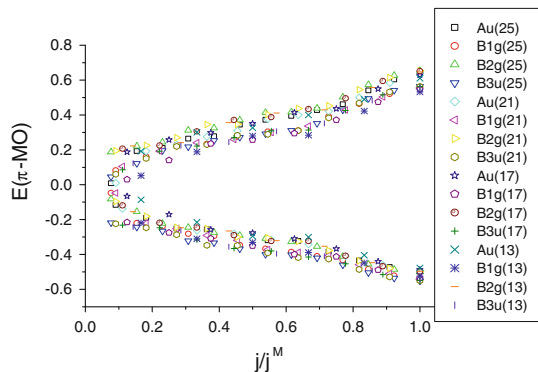
so the MOs belonging to the same irreducible representation are gathered and studied
to clarify the possible rules. In order to labeling the π-MOs of a particular irreducible
representation, we use j and j^M instead of J and J^M. Where the minuscule j denotes
the orbital number corresponding to the π-MOs belonged to a certain irreducible rep-
resentation, while the capital J denotes the orbital number of π-MOs belonged to the
four irreducible representations as a whole; and j^M denotes the largest absolute value
of j. Then, we use j/j^M to obtain the relation between the π-MO energy and j/j^M as
shown in Fig. 3.

From Fig. 3, the curves are approximately separated and symmetrically distrib-
uted about the non-bonding energy level. The energy sequence of π-MOs belonged
to different irreducible representations is:

$$E\left\{B_{2g}(V) \approx A_u(V)\right\} > E\left\{B_{1g}(V) \approx B_{3u}(V)\right\}$$
$$> E\left\{A_u(O) \approx B_{2g}(O)\right\} > E\left\{B_{1g}(O) \approx B_{3u}(O)\right\} \quad (6)$$

This sequence can clear be seen from any and alone zigzag graphenes. It should be
noted that: we adopt the absolute value of j/j^M for the abscissa in Fig. 3, so the OMO
and VMO all take positive value in the abscissa axis.

3.1.2 Fuzzy symmetry characteristics of the MOs in zigzag graphene about the translational transformation

Subsequently, we begin to explore the fuzzy symmetry of the MO in graphene molecule
about the space translational transformation. For zigzag graphene, it is expanded more
widely along the zigzag direction than the corresponding orthogonal direction. For
example, the mentioned four zigzag graphene molecules contain 6–12 benzene rings
along the horizontal direction, while they only have 3 benzene rings on the orthogonal
direction. Their membership functions of translational transformation about trans-
lating l periodic length along the zigzag direction ($\hat{T}_Z(l)$) are denoted as $MFT_Z l$.
Similarly, the membership functions of translational transformation about translating
l periodic length along the armchair direction ($\hat{T}_A(l)$) are denoted as $MFT_A l$. The
membership function of the MO obtained by Gaussian program can be calculated
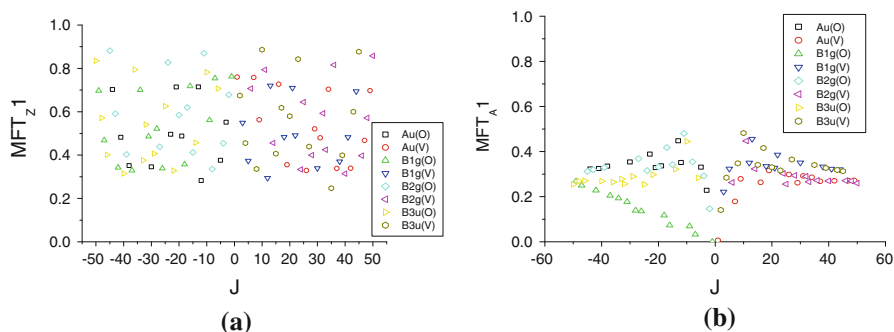
Fig. 4 Membership functions of the zigzag graphene $C_{100}H_{32}$ about translational transformation. **a** $C_{100}H_{32}$: $MFT_Z 1$ versus J. **b** $C_{100}H_{32}$: $MFT_A 1$ versus J

basing on the formula (5). For $C_{100}H_{32}$, its membership functions of translating 1 periodic lengths along the zigzag direction ($MFT_Z 1$) and along the armchair direction ($MFT_A 1$) are shown in Fig. 4a and b, respectively. It should be recalled that the periodic cell contains one benzene ring along the zigzag direction, while the periodic cell contains two benzene rings along the armchair direction.

We can find out that the value range of $MFT_Z 1$ is about 0.2–0.9, which is larger than that of $MFT_Z 2$ (0.3–0.8), corresponding figure being omitted. In addition, in Fig. 4a, for the OMO and VMO belonged to a given irreducible representation, their corresponding dots are approximately distributed in two "U-shaped" curves. The membership function ($MFT_A 1$) in Fig. 4b is for translating 1 periodic cell (two benzene rings) along the armchair direction. Because the molecule only contains three benzene rings at the armchair direction, the corresponding membership function is much smaller and usually under 0.5. More instructively, if we analyze the MO belonged to the same irreducible representation of D_{2h} point group by using the relative orbital number $j/abs(j^M)$, the similarity will be obvious at once as shown in Fig. 5, and in each panel the four zigzag graphenes are included.

From Fig. 5, it can be seen that for the four irreducible representations, the corresponding dots of $MFT_Z 1$ form four sets and are distributed in four U-shaped curves. As for different graphene molecules, the U-shaped curves of the same irreducible representation are very similar. Though there are two U-shaped curves for either OMO or VMO in the same irreducible representation, the pair of curves are not symmetrical distributed about the nonbonding MO (NBMO; $j/abs(j^M) = 0$). In addition, for the irreducible representation A_u, if we interchange the OMO with VMO (i.e. swapping the position of $-j$ and j), the transformed U-shaped curves of A_u could be almost superposed with that of B_{1g} as shown in Fig. 5. Analogously, the transformed U-shaped curves of B_{2g} are almost superposed with that of B_{3u}. In these irreducible representations, A_u and B_{1g} are a group, while B_{2g} and B_{3u} are another group. This is consistent with Fig. 3 and Eq. 6.

We can also do the analysis about $MFT_Z 2$ basing on the formula (5) and the corresponding curves. There is some similarity between $MFT_Z 2$ and $MFT_Z 1$, however, the number of U-shaped curves for each irreducible representation in $MFT_Z 2$ is more
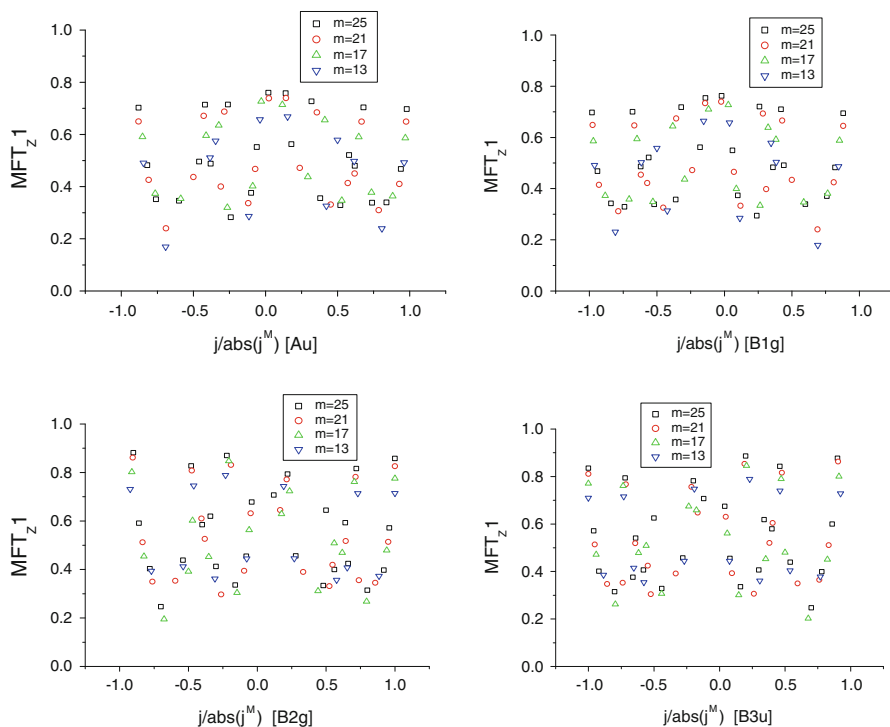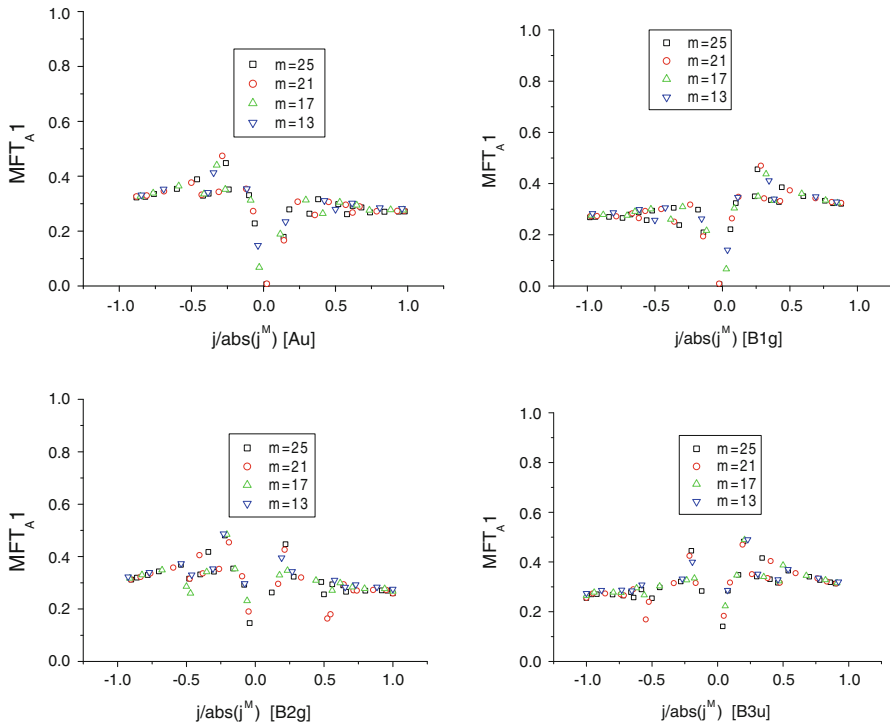
Fig. 5 MFT_Z1 versus $j/abs(j^M)$ of four irreducible representations belonged to D_{2h} point group in $C_{100}H_{32}$, $C_{84}H_{28}$, $C_{68}H_{24}$, and $C_{52}H_{20}$ (i.e. m = 25, 21, 17 and 13)

than 4. As for translational transformation of translating more periodic lengths ($l \geq 3$), the number of the U-shaped curves increases rapidly, which results in the reduction of the number of distributed dots and more difficult to distinguish these U-shaped curves. The relative figures are omitted for save space.

Then, we also investigated the membership functions of translating one periodic cell ($l = 1$) along the armchair direction based on the formula (5). The results of the above four graphene molecules are shown in Fig. 6. Because the translational periodic cell contains two benzene rings and the translational interval along the armchair direction is very short, the corresponding membership function is relatively small. Even so, the irreducible representations A_u and B_{1g} are a group; B_{2g} and B_{3u} are another group, which is similar as the analysis of MFT_Z1 and MFT_Z2.

3.2 Armchair graphene molecules

For comparison, armchair graphene molecules $C_{108}H_{32}$, $C_{72}H_{24}$, and $C_{36}H_{16}$ possessed D_{2h} point group symmetry are taken as examples to investigate. Their geometrical skeleton structures are similar to that of molecule $C_{200}H_{40}$ in Fig. 1. They all contain nine columns ($m = 9$) of C-atom, while the lines ($n = 4i$; $i = 3, 2, 1$) decrease in turn along the vertical direction, and similar as a homologues group. These three

Fig. 6 MFT_A1 versus $j/abs(j^M)$ of four irreducible representations belonged to D_{2h} point group in $C_{100}H_{32}$, $C_{84}H_{28}$, $C_{68}H_{24}$, and $C_{52}H_{20}$

molecules, respectively contain $9 \times 4i$ ($i = 3, 2, 1$) C-atoms and form $m \times n = 9n\pi$-MOs, in which the bonding occupied molecular orbitals (OMOs) and the anti-bonding vacant molecular orbitals (VMOs) each accounts for a half. According to the group theory, those π-MOs all possess D_{2h} point group symmetry and belong to some of the four irreducible representations: A_u, B_{1g}, B_{2g} and B_{3u}. Calculated by Gaussian program at the STO-3G level, we find that the numbers of those π-MOs belonged to different irreducible representations are $2n(A_u)$, $2n(B_{1g})$, $2.5n(B_{2g})$, and $2.5n(B_{3u})$, respectively.

3.2.1 Symmetry characteristics of the MO energy in armchair graphene

Similar with Sect. 3.1.1, we also plot the π-MO energies versus orbital number J for the three armchair graphene molecules, respectively and obtain for each molecule an approximate italic *S*-curve as shown in Fig. 7, where the abscissa is J, negative for the OMO and positive for the VMO. Similar to zigzag graphene, an energy gap between the OMO and VMO also appears for all armchair molecules. If we use the relative orbital number $J/abs(J^M)$ instead of the orbital number J, the corresponding energy dots of the three graphene will fall into the same italic *S*-curve similar as the zigzag molecules.

Fig. 7 π-MO energies of
armchair graphenes $C_{108}H_{32}$,
$C_{72}H_{24}$, and $C_{36}H_{16}$
(i.e. n = 12, 8, and 4)
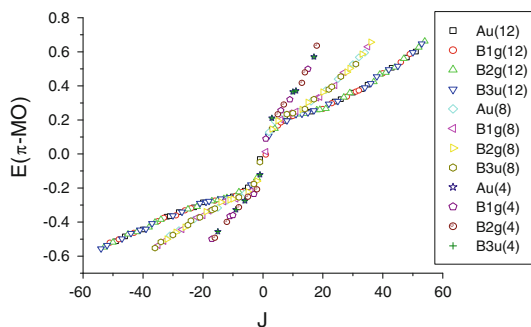
Fig. 8 π-MO energies of some
armchair grapheme
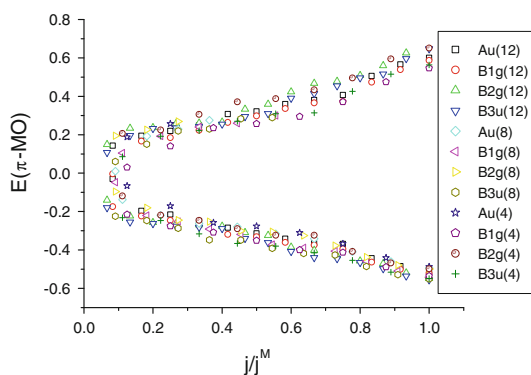
These π-MOs all possess D_{2h} point group symmetry and belong to one of the irreducible representations (A_u, B_{1g}, B_{2g}, and B_{3u}). In Fig. 8, π-MOs belonged to different irreducible representations are labeled by different symbols and number in the parentheses after the irreducible representations denotes the number of rows of C-atoms in each graphene. From Fig. 8, we can see that for one appointed armchair graphene, the energy dots corresponding to OMO and VMO are segregated in two sets but close to each other, forming approximately two separated branches. We have mentioned that for some conjugated molecules, such π-OMO or π-VMO branches correspond to the full band or the conduction band of the one-dimensional crystal, and the gap corresponds to the forbidden band gap [21,22]. Thus, it can be expected that an armchair graphene molecule containing a large quantity of C-atoms should also have electrical conductivity. However, contrasted with the zigzag graphene, the energy gap in armchair graphene is a little large. Perhaps this indicates that the electrical conductivity of armchair graphene is not as high as that of zigzag graphene, which is consistent with the known results [39,40].

By the way, we may also probe the molecular hardness (η) of the graphenes preliminary By using the principle of maximum hardness suggested by Parr and Pearson [41–43] and according to Koopmans's theorem [44], approximately, we can get:

$$\eta = (\varepsilon_{LUMO} - \varepsilon_{HOMO})/2 \tag{7}$$

So, a hard molecule ought to be the larger energy gap ($\varepsilon_{LUMO} - \varepsilon_{HOMO}$). Comparing the Figs. 2 and 7, perhaps, one may find that the molecular hardness of the armchair graphenes would be larger than that of the zigzag graphenes.

For these armchair graphene molecules, since they all possess D_{2h} point group symmetry, the π-MO energies of each of them can also be analyzed by the corresponding irreducible representations belonged to D_{2h} point group. Similar to zigzag graphene (see Fig. 3), Fig. 8 shows the plot for the π-MO energies of the three armchair graphenes. Comparing Fig. 3 with Fig. 8, we can see that the appearances of Figs. 3 and 8 are very similar. However, for single molecule, the dot distributions of OMO and VMO near the frontier MO are significantly different as shown in Figs. 3 and 8. In deed, it is very obvious that dots near the frontier MO are very sparse in Fig. 8 than that in Fig. 3, which suggests that the electrical conductivity of armchair graphene is lower than that of zigzag graphene. In fact, the results of tight binding approximation model suggest that: zigzag graphene shows the property of metal bond, while armchair graphene possesses the character of metal or semiconductor properties [39]. Density functional theory (DFT) calculations also show that the armchair graphene composing the graphene nano-ribbons has semiconductor property and its energy gap inversely proportions to the width of the graphene nano-ribbons [39]. The experimental results indeed confirm that energy gap will increase with the decrease of the width of the graphene nano-ribbons [40]. Therefore, our result seems reasonable.

3.2.2 Fuzzy symmetry characteristics of the MOs in armchair graphene about the translational transformation

In this section, the above three armchair graphene molecules are still taken as examples to discuss the fuzzy symmetry characteristics of this kind of molecules. For these armchair graphene molecules, there are 3–11 benzene rings in the armchair direction, while only 3–4 benzene rings along the orthogonal direction (namely, zigzag direction). Their membership functions of translational transformation about translating l periodic length along the zigzag direction ($\hat{T}_Z(l)$) are denoted as $MFT_Z l$. Similarly, the membership functions of translational transformation about translating l periodic length along the armchair direction ($\hat{T}_A(l)$) are denoted as $MFT_A l$. These membership functions of MOs obtained by Gaussian program can be calculated by using the formula (5). For $C_{108}H_{32}$, its membership functions of translating 1 periodic lengths along the zigzag direction (denoted as $MFT_Z 1$) and that along the armchair direction (denoted as $MFT_A 1$) are shown in Fig. 9a and b, respectively. The abscissa J and the meanings of other symbols are the same as that in Fig. 4. Here, the periodic cell contains one benzene ring when translating along the zigzag direction, while contains two benzene rings if translating along the armchair direction. Comparing the membership functions of the zigzag graphene with the armchair graphene about the translation transformation (Figs. 4, 9), there are some differences in their fuzzy symmetry characteristics.

Firstly, comparing Fig. 4a with Fig. 9a, though the molecular size and the number of π-MOs of $C_{100}H_{32}$ (zigzag graphene) are similar to $C_{108}H_{32}$ (armchair graphene), the translational distances along the zigzag direction, the resulting value intervals of $MFT_Z 1$ of zigzag $C_{100}H_{32}$ are all larger than that of armchair $C_{108}H_{32}$. In addition,
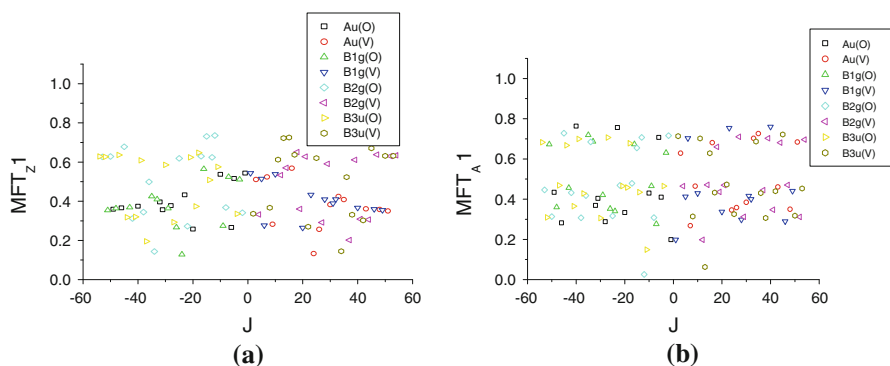
Fig. 9 Membership functions of the armchair graphene about translational transformation along the zigzag or armchair direction. **a** $C_{108}H_{32}$: MFT_Z1 versus J. **b** $C_{108}H_{32}$: MFT_A1 versus J

the U-shaped curve for the appointed irreducible representation in zigzag $C_{100}H_{32}$ is very obvious, but the curve in armchair $C_{108}H_{32}$ is hardly to see.

Secondly, for the MFT_A1 along the armchair direction (see Figs. 4b, 9b), the translational distance of the armchair graphen molecule is larger than that of the zigzag graphen. In Fig. 4b, the distribution of dots is lost the pattern of a U-shaped curve, but we can see this kind of curves appear though somewhat hazy in Fig. 9b. Because the translational range is small and molecular size is only about 5.5 times of the translating periodic cell, these U-shaped curves cannot be clearly seen.

We can also use the relative orbital number $j/abs(j^M)$ of the irreducible representations belonged to D_{2h} to analyze the membership functions of the three armchair graphene molecules as shown in Fig. 10 and the U-shaped curves are still discernible. From Fig. 10, for all of these four irreducible representations, we can obtain the U-shaped curves by using the MFT_A1 versus $j/abs(j^M)$ mapping their distribution relations. As for different graphene molecules, the U-shaped curves of the same irreducible representation look almost the same. But the two U-shaped curves corresponding to the OMO and VMO in the same irreducible representation are not symmetrical distributed about the NBMO. If we interchange the OMO with VMO (i.e. swapping the position of $-j$ and j), the transformed U-shaped curves of A_u could be almost superposed with that of B_{1g}. Similarly, the transformed U-shaped curves of B_{2g} are almost superposed with that of B_{3u}. If interchange the OMO with VMO (i.e. replacing j by $-j$), the U-shaped curves about A_u and B_{1g} may be almost interchangeable with each other. Similarly, these U-shaped curves of B_{2g} and B_{3u} may be also interchangeable. In the four irreducible representations, A_u and B_{1g} are a group, while B_{2g} and B_{3u} are another group.

3.3 Some other graphene molecules

In the above sections, a series of zigzag and armchair graphene molecules possessing D_{2h} point group symmetry are studied. However, there may be other point group symmetries in graphenes. Those point groups can be the subgroup of D_{2h}, or take D_{2h}
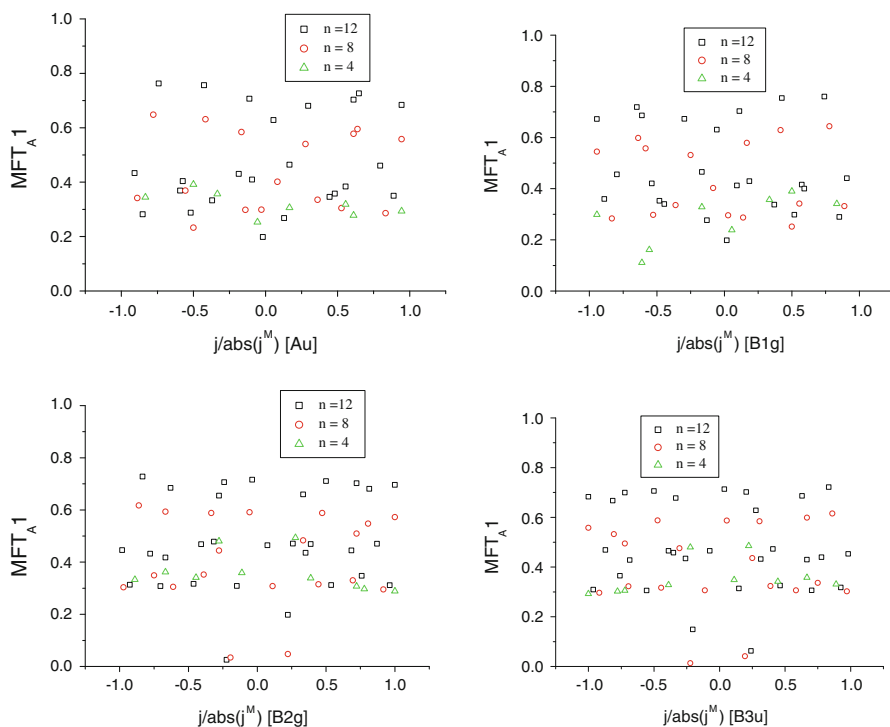
Fig. 10 $MFT_A 1$ versus $j/abs(j^M)$ of four irreducible representations belonged to D_{2h} point group in $C_{108}H_{32}$, $C_{72}H_{24}$ and $C_{36}H_{16}$

as their subgroup. In these two categories, we give some examples to be discussed, respectively.

3.3.1 Some zigzag graphene molecules possessing the symmetry of the subgroup of D_{2h}

In this section, two zigzag graphene isomers with the molecular formula $C_{94}H_{30}$ are investigated. They possess the symmetries of C_{2h} and C_{2v} (both the subgroup of D_{2h} point group) and denoted as $C_{94}H_{30}(C_{2h})$ and $C_{94}H_{30}(C_{2v})$, respectively. Their molecular structures are shown in Fig. 11. Note that the selection of the direction of coordinate axis in the Cartesian coordinates is based on the different point group of the molecule as shown in Fig. 11, by which we can determine the symbols of the irreducible representation of the related π-MO. This choice of coordinates is consistent with the coordinates provided by the Gaussian program. For the two molecules, their π-MOs belong to the irreducible representations A_u and B_g for $C_{94}H_{30}(C_{2h})$, while A_2 and B_1 for $C_{94}H_{30}(C_{2v})$, respectively.

Subsequently, we begin to discuss the π-MO energies and symmetries of the two zigzag graphene molecules. Their π-MO energies are showed in Fig. 12. Their relations between π-MO energy and orbital number J are similar to that in Fig. 2a of
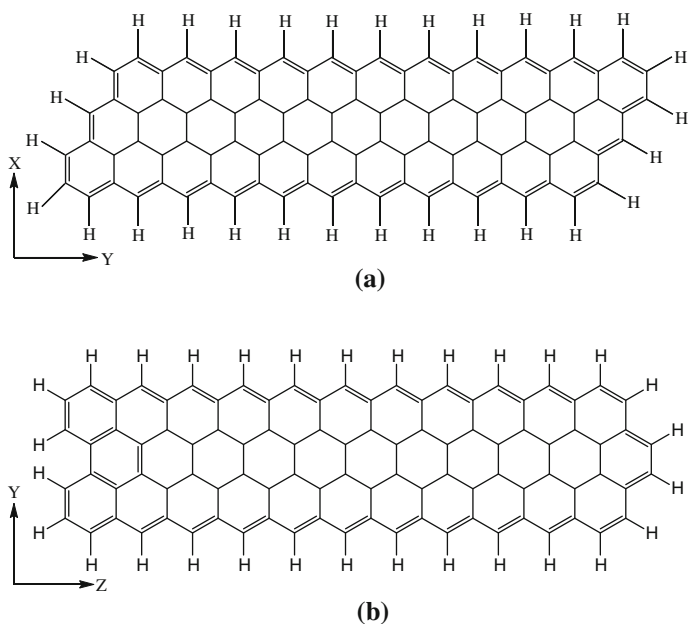
Fig. 11 Molecular structures of two zigzag graphene: **a** $C_{94}H_{30}$ (C_{2h}). Z axis (the direction of π-MO) is perpendicular to the paper plane and **b** $C_{94}H_{30}$ (C_{2v}). X axis (the direction of π-MO) is perpendicular to the paper plane
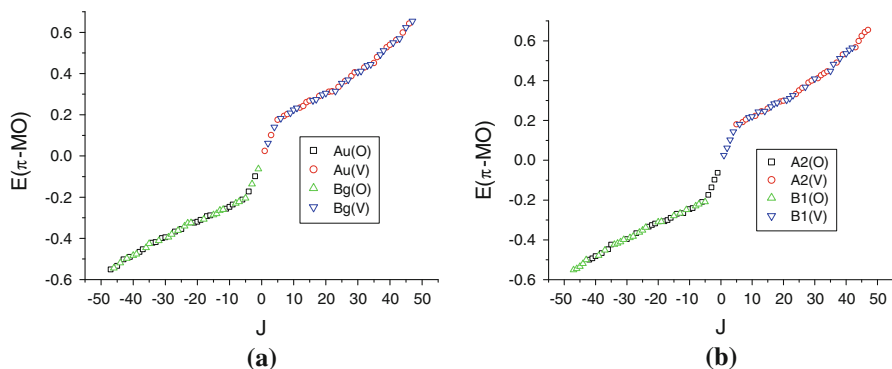

Fig. 12 π-MO energy versus J in **a** $C_{94}H_{30}$ (C_{2h}) and **b** $C_{94}H_{30}$ (C_{2v})

those D_{2h} molecules. However, these two molecules don't possess the perfect D_{2h} symmetry, and only have the fuzzy D_{2h} symmetry. Therefore, their π-MOs can't be simply classified by the four irreducible representations belonged to the D_{2h} point group, and should be classified by the irreducible representations belonged to C_{2h} and C_{2v}, namely (A_u, B_g) and (A_2, B_1), respectively.

Figure 13a and b show the membership functions of the two graphene molecules about translating one periodic cell along the zigzag direction, respectively. In Fig. 13, it can be seen that the points are symmetrical distributed about the NBMO.
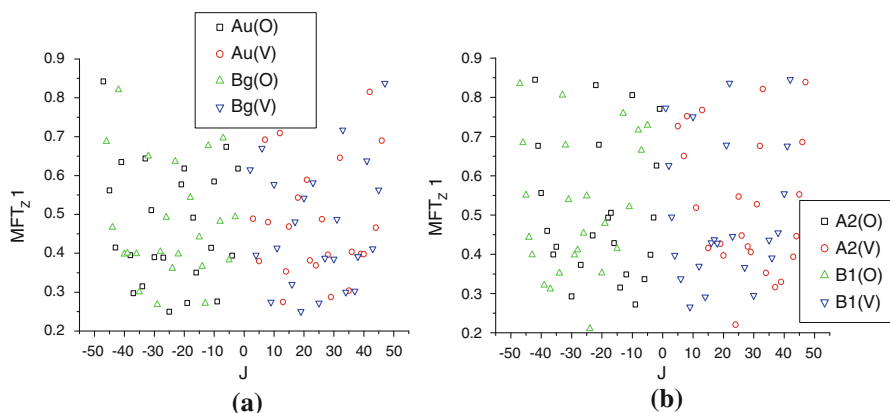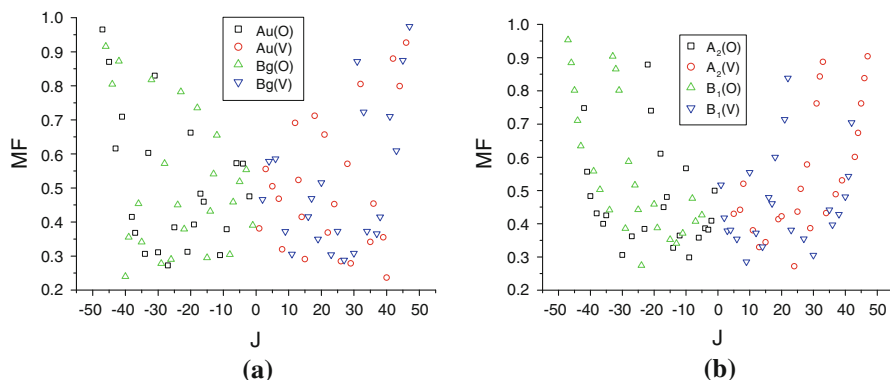
Fig. 13 MFT$_Z$1 versus J of **a** C$_{94}$H$_{30}$ (C$_{2h}$) and **b** C$_{94}$H$_{30}$ (C$_{2v}$) about translating one periodic length along the zigzag direction

The relationship between MFT$_Z$1 and orbital number J is similar to that of C$_{100}$H$_{32}$(D$_{2h}$) in Fig. 4a. However, the π-MOs of C$_{100}$H$_{32}$(D$_{2h}$) belong to four irreducible representations, and the π-MOs of C$_{94}$H$_{30}$ (C$_{2h}$) and C$_{94}$H$_{30}$ (C$_{2v}$) involve just two irreducible representations. So, there are four different irreducible representations in Fig. 4a, while only two in either Fig. 13a or b. Furthermore, In Fig. 4a, for C$_{100}$H$_{32}$ (D$_{2h}$), the distributions of the π-MOs belonged to B$_{3u}$ and B$_{1g}$ are in the similar curves (denoted as curves I), while the distributions of A$_u$ and B$_{2g}$ are in another similar curves (denoted as curves II), there are coincide with Eq. 6. For the π-MOs of C$_{94}$H$_{30}$ (C$_{2v}$), points of B$_1$ are distributed near the curves I; points of A$_2$ are distributed near the curves II as shown in Fig. 13b. As for the π-MOs of C$_{94}$H$_{30}$ (C$_{2h}$), the curves I and II both contain the relative points of A$_u$ and B$_g$ simultaneously, as shown in Fig. 13a. The reason for this interesting phenomenon can be found later text.

Because C$_{2h}$ and C$_{2v}$ are both the subgroup of D$_{2h}$, the fuzzy symmetry of graphenes C$_{94}$H$_{30}$ (C$_{2h}$) and C$_{94}$H$_{30}$ (C$_{2h}$) can be analyzed by the D$_{2h}$ point group. Their irreducible representations of the π-MOs can be expressed by the superposition of two relevant irreducible representations of D$_{2h}$ point group. According to the fuzzy symmetry theory [12,13], it can be determined by the membership functions of the π-MO through a two-fold symmetry transformation. This kind of symmetry transformation exists in the D$_{2h}$ point group, but not in its subgroup. For example, for the π-MO of C$_{94}$H$_{30}$ (C$_{2h}$), the two-fold symmetry transformation can be the mirror reflect transformation (see Fig. 11a, where the xy plane as the mirror M$_1$), or the central inversion transformation, which can not be of C$_{94}$H$_{30}$ (C$_{2v}$). On the other hand, for the π-MO of C$_{94}$H$_{30}$ (C$_{2v}$), such two-fold symmetry transformations can be any one of the mirror reflect transformations(see Fig. 11b) which may be not of C$_{94}$H$_{30}$ (C$_{2h}$).

Corresponding to the transformations in D$_{2h}$ not in C$_{2h}$, the same membership function of the π-MO of C$_{94}$H$_{30}$ (C$_{2h}$) versus its orbital number J is obtained and plotted in Fig. 14a. In Fig. 14a, all the dots near symmetrically distributed about the NBMO. For the same J, the membership function (MF) values of the OMO-J and VMO-J are similar, but they belong to different irreducible representations, that is, the dots for

Fig. 14 MF versus J (π-MO of **a** $C_{94}H_{30}$ (C_{2h}) and **b** $C_{94}H_{30}$ (C_{2v}) about a certain twofold symmetry transformations in D_{2h}

A_u and B_g are near symmetrically distributed about the NBMO. For example, for the pair of dots $J = -47$(the minimum J) and $J = 47$(the maximum J), the corresponding membership functions of $A_u(O)$ and $B_g(V)$ are both about 0.95.

As for the π-MO of $C_{94}H_{30}$ (C_{2v}), the relevant plot of membership function of the π-MO of $C_{94}H_{30}$ (C_{2v}) versus orbital serial number J, according to the transformations in D_{2h} not in C_{2v}, can be drawn and shown in Fig. 14b. In Fig. 14b, we can see that the dots also near symmetrically distributed about the NBMO and for the same J, the MF values of OMO-J and VMO-J are nearly the same, but their relevant irreducible representations are different. The dots for A_2 and B_1 are also near symmetrically distributed about the NBMO. This is similar to the results in Fig. 14a.

There are two correlative but distinct physical entity in molecular symmetry theoretical studies: the symmetry and conservation quantity, specifically, the molecular point group and the irreducible representation of the related MOs (i.e. its characteristics) [45]. The corresponding physical entity in the study of molecular fuzzy symmetry are the membership functions and irreducible representation components [12,13]. For the two-fold symmetry transformation, $\hat{G}_2$, its corresponding combination coefficients for irreducible representation components are the symmetrical components X_S and the anti-symmetrical components X_A. If their corresponding irreducible representations are denoted as $\Gamma(S)$ and $\Gamma(A)$, respectively, the membership function of MO is:

$$\Gamma = X_S\Gamma(S) + X_A\Gamma(A) \tag{8}$$

Similarly, for the π-MOs of $C_{94}H_{30}$ (C_{2h}), the irreducible representations A_u and B_g of C_{2h} point group can be expressed as:

$$\Gamma(A_u/C_{2h}) = X(A_u/D_{2h})\Gamma(A_u/D_{2h}) + X(B_{3u}/D_{2h})\Gamma(B_{3u}/D_{2h}) \tag{8a}$$
$$\Gamma(B_g/C_{2h}) = X(B_{2g}/D_{2h})\Gamma(B_{2g}/D_{2h}) + X(B_{1g}/D_{2h})\Gamma(B_{1g}/D_{2h}) \tag{8b}$$

where the symbols, before and after the '/' in the parenthesis, represent the irreducible representation and its originating point group, respectively. When we choose the
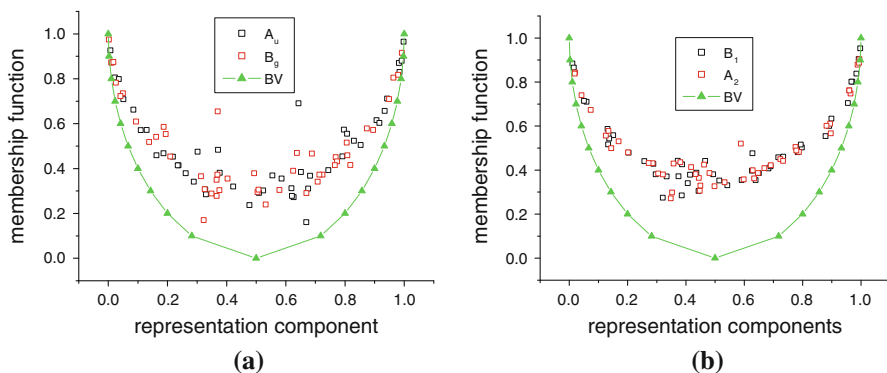
Fig. 15 Membership function versus irreducible representation in **a** $C_{94}H_{30}$ (C_{2h}) and **b** $C_{94}H_{30}$ (C_{2v})

two-fold symmetry transformation mentioned above, formulas (8a) and (8b) both establish. Of course, among the irreducible representations of D_{2h}, the symmetrical and the anti-symmetrical irreducible representations may be altered, but the final formulas (8a) and (8b) will still be the same. Thus, we can calculate the coefficients of the irreducible representation components for the π-MO in the D_{2h}, based on the fuzzy symmetry theoretical methods [12,13]. Similarly, for the π-MOs of $C_{94}H_{30}$ (C_{2v}), the irreducible representations A_2 and B_1 of C_{2v} can be expressed as:

$$\Gamma(A_2/C_{2v}) = X(A_u/D_{2h})\Gamma(A_u/D_{2h}) + X(B_{2g}/D_{2h})\Gamma(B_{2g}/D_{2h}) \tag{9a}$$

$$\Gamma(B_1/C_{2v}) = X(B_{1g}/D_{2h})\Gamma(B_{1g}/D_{2h}) + X(B_{3u}/D_{2h})\Gamma(B_{3u}/D_{2h}) \tag{9b}$$

Note that the irreducible representation A_2 of C_{2v} in formula (9a) is the combination of the A_u and B_{2g} of D_{2h} point group. In Fig. 14b, for the π-MOs of $C_{94}H_{30}$ (C_{2v}), the dots of the A_2 are distributed in curves II. As for the π-MOs of $C_{100}H_{32}$, the dots of the A_u and B_{2g} are also distributed in curves II as shown in Fig. 4a. This is consistent with the $C_{94}H_{30}$ (C_{2v}). Similarly, for the π-MOs of $C_{94}H_{30}$ (C_{2v}), the dots of the B_1 are distributed in a set of curves I basing on the formula (9b), which is consistent with that of B_{1g} and B_{3u} in $C_{100}H_{32}$ as shown in Fig. 4a. Based on (8a) and (8b), it is not hard to explain why the dots of A_u and B_g of $C_{94}H_{30}$ (C_{2h}) may be distributed in the two curve sets (I or II), simultaneously.

Moreover, based on the fuzzy symmetry theoretical methods [12,13], we can obtain the irreducible representation components for the relevant π-MO of the D_{2h} point group. We may show the relations between the components of the irreducible representation and the orbital number J in $C_{94}H_{30}$ (C_{2h}) and $C_{94}H_{30}$ (C_{2V}) molecules, easily.

Because there is a certain dependence between the membership function of π-MO and the irreducible representation components [13,20,21], we can plot the membership functions of the π-MOs in $C_{94}H_{30}$ (C_{2h}) and $C_{94}H_{30}$ (C_{2V}) versus the corresponding irreducible representations components, as shown in Fig. 15a and b. The ordinate is the membership functions of π-MO about the mentioned two-fold symmetry transformation in the subgroup of D_{2h}. For $C_{94}H_{30}$ (C_{2h}), as shown in Fig. 15a, the abscissa of

the π-MOs belonging to the irreducible representation A_u/C_{2h} is $X(B_{3u}/D_{2h})$ and that of π-MOs belonging to the irreducible representation B_g/C_{2h} is $X(B_{2g}/D_{2h})$. As for $C_{94}H_{30}$ (C_{2v}), the abscissa of the π-MOs belonging to the irreducible representation B_1/C_{2v} is $X(B_{3u}/D_{2h})$ and that of π-MOs belonging to the irreducible representation A_2/C_{2h} is $X(B_{2g}/D_{2h})$ as shown in Fig. 15b. By the way, in Fig. 15, the boundary value (BV) curve [20] limits the area where all the points will appear.

3.3.2 Graphene molecule possessing the D_{6h} symmetry

In this section, we begin to discuss the graphene molecule possessing D_{6h} symmetry. The coronene-$C_{96}H_{24}$ may be shown as the example in Fig. 16. It contains 96 π-MOs, including 48 bonding π-MOs and 48 anti-bonding π-MOs. These π-MOs belong to the irreducible representations of D_{6h} point group, which include 5 kinds of one-dimensional irreducible representations (A_{1u}, A_{2u}, B_{1g}, B_{2g}, and B_{3u}) and 2 kinds of two-dimensional irreducible representations (E_{1g} and E_{2u}).

The π-MO energies of $C_{96}H_{24}$ molecule are shown in Fig. 17, in which Fig. 17a exhibits the relation between π-MO energy and orbital number J; Fig. 17b and c show the relation between π-MO energies of one-dimensional and two-dimensional irreducible representations and the relative orbital number j/j^M, respectively. These figures are generally similar to the results of the earlier discussed graphene molecules, however there are some distinct features. From Fig. 17a, it can be seen that the gap between the OMO and VMO is larger, which suggests its electrical conductivity may be weaker than that of the graphene discussed formerly. Because some of the π-MOs belong to one-dimensional irreducible representations and the others belong to two-dimensional irreducible representations, we use the E(π-MO) versus (j/j^M) draw figures shown in Fig. 17b and c, respectively. Generally speaking, these figures are similar to that of the earlier discussed graphenes. The corresponding dots are symmetrically distributed about the NBMO. Note that in Fig. 17c, the MOs belonging to

**Fig. 16** Molecule structure of $C_{96}H_{24}$
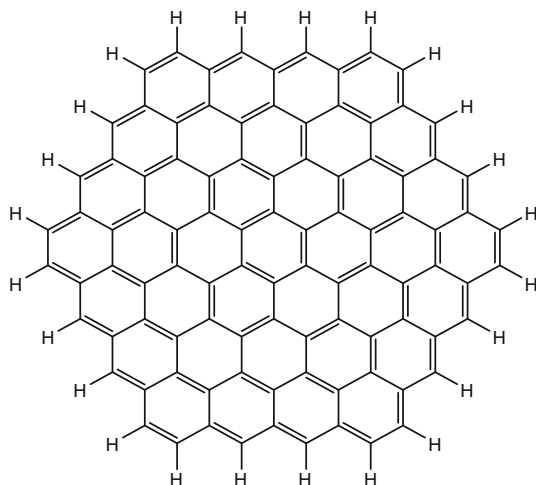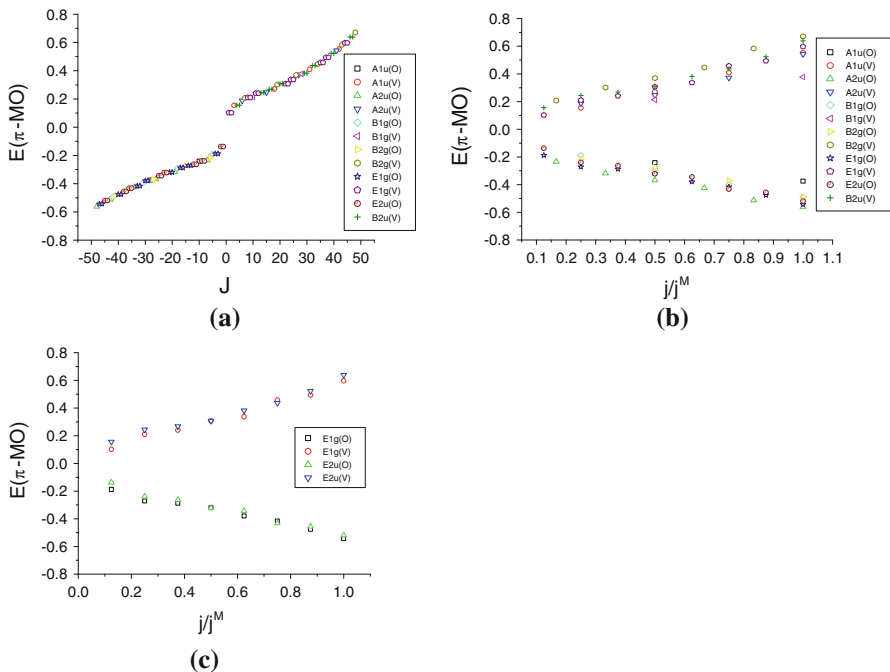
Fig. 17 π-MO energy versus J in $C_{96}H_{24}$ (D_{6h}): **a** π-MO energy versus J(a); **b** π-MO energy versus j/j^M of one-dimensional irreducible representations; **c** π-MO energy versus j/j^M of two-dimensional irreducible representations

two-dimensional irreducible representations are two-fold degenerate, so each point in the figure represents two π-MOs and the choice of the MOs may different. Usually, each of the individual MO alone does not have all of the symmetries corresponding to D_{6h}, only the whole set of the two MOs can have those symmetries and the membership functions (taking the sum of squares of the LCAO coefficients from every MO attributed by the atom as the criterion of the atom) of all the symmetry transformations of D_{6h} point group can be equal to one, while for single MO, the membership function of some symmetry transformations in D_{6h} is less than one. These results have been discussed in our analysis of the fuzzy symmetry of benzene [16] and the calculations for $C_{96}H_{24}$ (D_{6h}) molecule are similar, so the analogous calculations are omitted here.

As for the membership function of translating one periodic length along the zig-zag direction (MFT_Z1) in $C_{96}H_{24}$ (D_{6h}) molecule is shown in Fig. 18. Similar to the discussion in the previous mentioned graphenes, the dots distribution is symmetrical about the NBMO, and the points in the symmetrical positions also belong to different irreducible representations. In addition, since quite a lot of MOs belong to two-dimensional irreducible representations, they are twofold degenerate. The MFT_Z1 values of these degenerate MOs are also degenerate. Figure 18 shows pairs of two adjacent equivalent points. Though the pair of degenerate MO can be selected in many different ways, which may result in the value of MFT_Z1 different, the MOs are always degenerate and their MFT_Z1 should be the same value for their MO set as a whole.

Fig. 18 $MFT_Z 1$ versus J
in $C_{96}H_{24}$ (D_{6h})
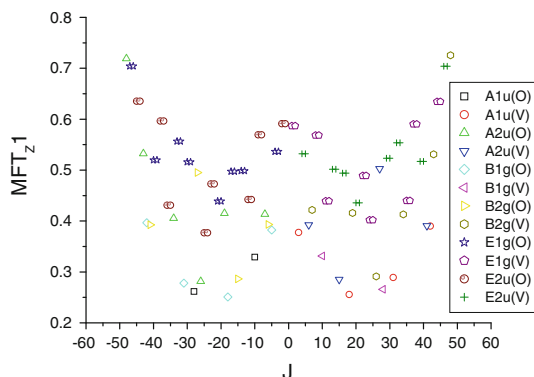
4 Conclusions

Generally speaking, graphene molecules can be regarded as fuzzy layer group (G_2^n)
systems, which present periodic or fuzzy periodic translational symmetry in two inde-
pendent directions. The preferable choice is along the zigzag direction and the arm-
chair direction. So, we take some typical graphene molecules as examples to discuss
their symmetries and fuzzy symmetries, π-MO energies, the irreducible representa-
tion components, and the membership functions about the relevant space translational
symmetry transformation. The main conclusions obtained are summarized as follows:

(1) Analyzed a set of zigzag graphenes $C_{100}H_{32}$, $C_{84}H_{28}$, $C_{68}H_{24}$, and $C_{52}H_{20}$ pos-
sessing the D_{2h} symmetry. In the plot of π-MO energy versus J (serial number of
π-MO), the dots are all distributed forming italic S-shaped curves with approx-
imately central symmetry, and a small gap in each curve can be regarded as the
NBMO energy level. For these zigzag graphenes, their membership functions of
translating one periodic cell along zigzag direction $\hat{T}_Z(l)$ are also analyzed. As
for the appointed irreducible representation of OMO and VMO, the relative dots
are distributed in two U-shaped curves. When we use relative orbital number
instead of J, these U-shaped curves are almost the same for different molecules.

(2) A group of armchair graphene molecules $C_{108}H_{32}$, $C_{72}H_{24}$, $C_{36}H_{16}$ with D_{2h}
symmetry are taken as typical examples. The plot of $E(\pi$-MO) versus J are sim-
ilar to that of zigzag graphene molecules. The main difference is that the energy
gap between OMO and VMO in armchair graphene is significantly larger than
that of the zigzag graphene. Maybe, the molecular hardness of armchair graphene
is also larger than that of zigzag graphene. For these graphenes, their membership
functions of translating one periodic cell along the armchair direction $\hat{T}_Z(l)$ are
also analyzed. The plots of $MFT_A 1$ versus J are similar to that of $MFT_Z 1$ versus
J of zigzag graphene molecules. However, the main difference with the zigzag
graphene is that the relationship of $MFT_A 1$ versus J is not as obvious as in zigzag
graphene.

(3) Two zigzag graphene isomers $C_{94}H_{24}$ (C_{2h}) and $C_{94}H_{24}$ (C_{2v}) possessing sub-
group symmetry of D_{2h} are discussed. In plot of $E(\pi$-MO) versus J and $MFT_Z 1$

versus J, the obtained curves are approximately similar to that of the graphene molecules of D_{2h} symmetry, but the irreducible representations of the π-MOs can only be determined according to the subgroup of D_{2h}. Nevertheless, we can analyze the fuzzy symmetries of their π-MOs according to the D_{2h} point group and obtain the components of their corresponding irreducible representations and membership functions, as well as the correlation between them.

(4) Molecule $C_{96}H_{24}$ possessing the symmetry of D_{6h} point group is briefly discussed as well as the relationship between plots of $E(\pi$-MO) versus J and MFT_Z1 versus J. Because D_{6h} point group possesses higher symmetry and D_{2h} is its subgroup, their π-MOs can belong not only to the one-dimensional irreducible representations, but also to two the two-dimensional irreducible representations. The π-MOs of two-dimensional irreducible representations are all two-fold degenerate with the same energy level and the same membership function values. However, the two degenerate π-MOs can be selected in different ways, the membership function MFT_Z1 of the whole π-MO set ought to be always equal one.

References

1. P.G. Mezey, J. Maruani, Mol. Phys. **69**(1), 97–113 (1990)
2. P.G. Mezey, J. Maruani, Int. J. Quantum Chem. **45**(2), 177–187 (1993)
3. P.G. Mezey, J. Math. Chem. **23**(1), 65–84 (1998)
4. J. Maruani, P.G. Mezey, Le concept de"syntopie": une extension continue du concept de symétrie pour des structures quasi-symétriques à l'aide de la méthode des ensembles flous. Compt. Rend. Acad. Sci. Paris (Série II) **305**, 1051–1054 (1987)
5. J. Maruani, A. Toro-Labbé, Le modèle de la syntopie et l'état de transition de réactions chimiques: fonctions d'appartenance et coefficients de Brönsted pour l'isomérisation cis-trans. Compt. Rend. Acad Sci. Paris (Série IIb) **323**, 609–615 (1996)
6. P.G. Mezey, Int. Rev. Phys. Chem. **16**, 361–388 (1997)
7. H. Zabrodsky, S. Peleg, D. Avnir, J. Am. Chem. Soc. **115**, 8278–8289 (1993)
8. D. Avnir, H. Zabrodsky, H. Hel-Or, P.G. Mezey, Symmetry and chirality: continuous measures. Ncyclop. Comput. Chem. **4**:2890–2901 (1998) ed by Paul von Ragué Schleyer, (Wiley, Chichester)
9. R. Chauvin, Chemical algebra. I: fuzzy subgroups. J. Math. Chem. **16**(1), 245–256 (1994)
10. R. Chauvin, Chemical algebra. II: discriminating pairing products. J. Math. Chem. **16**(1), 257–258 (1994)
11. X.Z. Zhou, Z.X. Fan, J.J. Zhan, *Application of Fuzzy Mathematics in Chemistry* (National University of Defence Technology Press, Changsha, 2002), pp. 325–349
12. X.Z. Zhao, X.F. Xu, Acta Phys. Chim. Sci. **20**, 1175 (2004)
13. X.Z. Zhao, X.F. Xu, G.C. Wang, Y.M. Pan, Z.S. Cai, Mol. Phys. **103**(24), 3233–3241 (2005)
14. X.F. Xu, G.C. Wang, X.Z. Zhao, Y.M. Pan, Y.Y. Liang, Z.F. Shang, J. Math. Chem. **41**(2), 143–160 (2007)
15. X.Z. Zhao, X.F. Xu, G.C. Wang, Y.M. Pan, Z.F. Shang, R.F. Li, J. Math. Chem. **42**(2), 265–288 (2007)
16. X.Z. Zhao, G.C. Wang, X.F. Xu, Y.M. Pan, Z.F. Shang, R.F. Li, Z.C. Li, J. Math. Chem. **43**(2), 485–507 (2008)
17. X.Z. Zhao, Z.F. Shang, G.C. Wang, X.F. Xu, R.F. Li, Y.M. Pan, Z.C. Li, J. Math. Chem. **43**(3), 1141–1162 (2008)
18. X.Z. Zhao, Z.F. Shang, H.W. Sun, L. Chen, G.C. Wang, X.F. Xu, R.F. Li, Y.M. Pan, Z.C. Li, J. Math. Chem. **44**(1), 46–74 (2008)
19. X.Z. Zhao, X.F. Xu, Z.F. Shang, G.C. Wang, R.F. Li, Acta Phys. Chim. Sci. **24**(5), 772–780 (2008)
20. X.Z. Zhao, Z.F. Shang, Z.C. Li, X.F. Xu, G.C. Wang, R.F. Li, Y. Li, J. Math. Chem. **48**(2), 187–223 (2010)
21. Y. Li, X.Z. Zhao, X.F. Xu, Z.F. Shang, Z.S. Cai, G.C. Wang, R.F. Li, Science in China Ser. B-Chem **52**(11), 1892–1910

22. X.Z. Zhao, *Molecular Symmetry and Fuzzy Symmetry* (Nova Sci. Publishers Inc, NY, 2010)
23. S.K. Xing, Y. Li, X.Z. Zhao, Z.F. Shang, X.F. Xu, Z.S. Cai, G.C. Wang, R.F. Li, Acta Phys. Chim. Sin. **26**(7), 1947–1958 (2010)
24. R.H. Wang, K.X. Gao, *Symmetry Group of Crystallography (in Chinese)* (Science Press, Beijing, 1990)
25. B.K. Vainshtein, *Modern Crystallography I, Symmetry of Crystals, Methods of Structural of Crystallography* (Springer, Berlin, 1981)
26. J.A. Rogers, Nat. Nanotechnol. **3**, 254 (2008)
27. G. Brumfiel, Nature **458**, 390 (2009)
28. K.S. Novoselov, A.K. Geim, S.V. Morozov, D. Jiang, Y. Zhang, S.V. Dubonos, I.V. Grigoreva, A.A. Firsov, Science **306**, 666 (2004)
29. C.G. Lee, X.D. Wei, J.W. Kysar, J. Hone, Science **321**, 385 (2008)
30. Y. Zhang, Y.-W. Tan, H.L. Stormer, P. Kim, Nature **438**, 201 (2005)
31. L.A. Ponomarenko, F. Schdin, M.I. Katsnelson, R. Yang, E.W. Hill, K.S. Novoselov, A.K. Geim, Science **320**, 324 (2008)
32. E.J. Kan, Z.Y. Li, J.L. Yang, Nano **3**, 433 (2009)
33. J.A. Matthew, C.T. Vincent, B.G. Richard, Chem. Rev. **110**, 132–145 (2010)
34. C.N.R. Rao, A.K. Sood, K.S. Subrahmanuyam, A. Govindaraj, Angew. Chem. Int. Ed. **48**, 7752–7777 (2009)
35. H. Rainer, Chem. Rev. **106**, 4820–4842 (2006)
36. S.K Xing, Y. Li, X.Z. Zhao, Z.S. Cai, Z.F. Shang, G.C. Wang, Acta Phys. Chim. Sin. **27**(5), 1000–1004 (2011)
37. M.A. Armstrong, *Basic Topology* (Springer Science+Business Media Inc, NY, 1983)
38. M.J. Frisch, G.W. Trucks, H.B. Schlegel et al., *Gaussian 03, Revision B.01*. Gaussian, Inc., Pittsburgh (1998)
39. V. Barone, O. Hod, G.E. Scuseria, Nano Lett. **6**(12), 2748 (2006)
40. M.Y. Han, B. Özyilmaz, Y. Zhang, P. Kim, Phys. Rev. Lett. **98**, 206805 (2007)
41. R.G. Parr, R.G. Pearson, J. Am. Chem. Sco. **105**, 7512–7516 (1983)
42. R.G. Pearson, Acc. Chem. Res. **26**, 250–255 (1993)
43. R.G. Pearson, Z.X. Zhou, Acc. Chem. Res. **26**, 256–258 (1993)
44. T. Kart, S. Scheiner, J. Phys. Chem. **99**, 8121–8124 (1995)
45. X.Z Zhao, Z.S. Cai, G.C. Wang, Y.M. Pan, B.X. Wu, J. Mol. Struct. (THEOCHEM) **586**, 209–223 (2002)